Science
AAAS

Tuned for Transposition: Molecular Determinants Underlying the Hyperactivity of a Stowaway MITE

Guojun Yang, *et al.*

Science **325**, 1391 (2009);
DOI: 10.1126/science.1175688

Tuned for Transposition: Molecular Determinants Underlying the Hyperactivity of a *Stowaway* MITE

Guojun Yang,[1,2,3] Dawn Holligan Nagel,[1] Cédric Feschotte,[4] C. Nathan Hancock,[1] Susan R. Wessler[1]*

Miniature inverted repeat transposable elements (MITEs) are widespread in eukaryotic genomes, where they can attain high copy numbers despite a lack of coding capacity. However, little is known about how they originate and amplify. We performed a genome-wide screen of functional interactions between *Stowaway* MITEs and potential transposases in the rice genome and identified a transpositionally active MITE that possesses key properties that enhance transposition. Although not directly related to its autonomous element, the MITE has less affinity for the transposase than does the autonomous element but lacks a motif repressing transposition in the autonomous element. The MITE contains internal sequences that enhance transposition. These findings suggest that MITEs achieve high transposition activity by scavenging transposases encoded by distantly related and self-restrained autonomous elements.

Most eukaryotic genomes contain large numbers of many different types of transposable elements (TEs). The vast majority of these TEs cannot replicate and mobilize themselves into new regions of the genome (they are nonautonomous). These elements thus depend on transposases encoded by other, autonomous, elements. Miniature inverted repeat TEs (MITEs) are a type of nonautonomous element found in both prokaryotic and eukaryotic genomes, where they are often located in or near genes (*1*–*3*). MITEs resemble typical DNA transposons, although they tend to have a small size [<500 base pairs (bp)] and high copy number and contain terminal inverted repeats (TIRs) flanked by target site duplications. Although MITEs lack coding capacity, in plants they are classified as either *Tourist*-like or *Stowaway*-like (*4*). Although the high copy numbers of MITEs in plant genomes suggest that they have high transposition activity, only the *Tourist*-like rice element *mPing*, an internal deletion derivative of its autonomous partner *Ping*, has been shown to be currently active (*5*–*7*). However, the mechanism by which rice strains accumulate 100- to 1000-fold more *mPing* than *Ping* elements is unknown (*8*).

Unlike *mPing*, the vast majority of characterized MITEs are not deletion derivatives of existing autonomous transposons (*9*, *10*). Furthermore, because none of these MITEs are active, their origin, success, and source of transposase have been a mystery. The most logical model to explain the movement of these nondeletion derivative MITEs is that they can borrow the transposase of distantly related elements (in a process referred to as cross-mobilization) and amplify within the genome (*4*).

The sequenced genome of *Oryza sativa* (rice) contains more than 22,000 *Stowaway* MITEs belonging to at least 25 subfamilies (*10*). Furthermore, the structure of MITE phylogenetic trees indicates that subfamilies are derived from the amplification of one or a few individual elements to hundreds or thousands of copies (*10*). *Stowaway* elements have not previously been shown to be active in rice or in any other genome. Surprisingly, none of the *Stowaway* families appeared to be deletion derivatives of any transposase-encoding element found within sequenced rice genomes. It was predicted that rice *Mariner*-like elements (called *Osmar*s) were the most likely source of transposase because *Stowaway* and *Osmar* share

[1]Department of Plant Biology, University of Georgia, Athens, GA 30602, USA. [2]Department of Biology, University of Toronto at Mississauga, Mississauga, ON L5L 1C6, Canada. [3]Cell and Systems Biology, University of Toronto, Toronto, ON M5S 3G5, Canada. [4]Department of Biology, University of Texas at Arlington, Arlington, TX 76019, USA.

*To whom correspondence should be addressed. E-mail: sue@plantbio.uga.edu

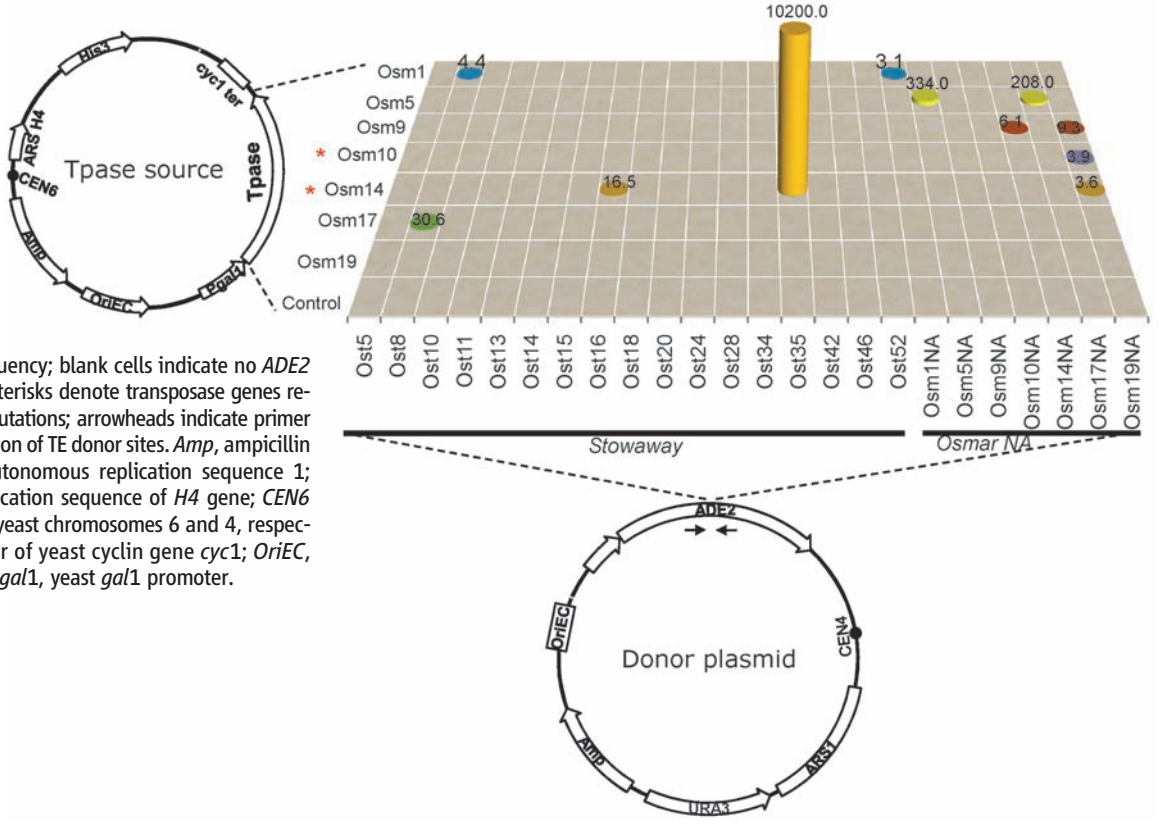

Fig. 1. Yeast excision assay. *Stowaway*s (Osts) and nonautonomous *Osmar*s (OsmNAs) cloned into the *ade*2 coding sequence are shown on the *x* axis; *Osmar* transposases are shown on the *y* axis; and *ADE2* reversion frequency (10^{-9} per cell) (table S1) is shown on the *z* axis. Numbers on cylinders show average *ADE2* reversion frequency; blank cells indicate no *ADE2* reversion was detected. Asterisks denote transposase genes repaired for frame-shifting mutations; arrowheads indicate primer positions for PCR amplification of TE donor sites. *Amp*, ampicillin resistance gene; *ARS1*, autonomous replication sequence 1; *ARS H4*, autonomous replication sequence of *H4* gene; *CEN6* and *CEN4*, centromeres of yeast chromosomes 6 and 4, respectively; *cyc*1 ter, terminator of yeast cyclin gene *cyc*1; *OriEC*, *E. coli* replication origin; P*gal*1, yeast *gal*1 promoter.

terminal inverted repeats (of ~10 bp) and the same target site duplication (the dinucleotide TA) (fig. S1).

On the basis of their transposase protein sequences, *Osmar*s were classified into 25 families and placed in three major clades (*10*). Among the 34 *Osmar*s, only five contain intact transposase-coding regions. Here, we refer to *Osmar*s with complete ends and intact coding sequences as potentially autonomous elements, those with mutated or truncated coding sequences as nonautonomous elements, and small elements lacking any coding sequences as deletion derivatives of *Osmar* (fig. S1).

To determine whether any *Osmar* transposases could catalyze the transposition of rice *Stowaway* MITEs, we modified a yeast assay previously developed to demonstrate transposition of a nonautonomous version of *Osmar*5 (Osm5NA) by its own transposase (*11*). The assay has two plasmid components (Fig. 1): One is a transposase (Tpase) source that expresses one of seven *Osmar* transposases (abbreviated Osm1, Osm5…) representing each *Osmar* subclade under the control of an inducible yeast promoter (P*gal1*) (*12*). The second plasmid in our assay contains the *ade2* reporter gene disrupted by one of 24 nonautonomous elements, including 17 *Stowaway*s (abbreviated Ost5, Ost8…) chosen to represent the diversity of *Stowaway* families in rice, and seven direct-deletion derivatives of each *Osmar* element (abbreviated OsmXNA, where NA means nonautonomous) (*12*). In yeast cells containing both plasmids, potentially successful transposase-transposon interactions were scored on the basis of *ADE2*-revertant colonies (Fig. 1).

These tests revealed that six of the seven transposases showed evidence of activity and uncovered several instances of cross-mobilization (Fig. 1 and table S1). The nonautonomous versions of *Osmar*1 and *Osmar*5 (Osm1NA and Osm5NA) were excised in the presence of their cognate transposases, and cross-mobilization occurred for Osm17NA by Osm5; Osm19NA by Osm9, Osm10, and Osm14; and Osm14NA by Osm9. We also identified interactions between three *Stowaway* elements and *Osmar* transposases: Ost8 by Osm1 and Osm17, and Ost16 and Ost35 by Osm14 (Fig. 1 and table S1). In contrast to the low excision activities observed for Ost8 and Ost16, the excision of Ost35 by Osm14 was the highest interaction recorded by this assay (Fig. 1 and fig. S2A). Polymerase chain reaction (PCR) amplification confirmed independent excision events of Ost35 by the *Osmar*14 transposase (fig. S2B), and sequencing of the PCR products revealed excision footprints (fig. S2C) similar to those retrieved for *Osmar*5 in this and a previous study (fig. S3A) (*11*). Additionally, reinsertions of Ost35 into chromosomal loci were confirmed by means of Southern hybridization of yeast genomic DNA (figs. S2D and S3B). The fact that *Stowaway*s were mobilized by *Osmar* transposases provides a functional mechanism for the mobilization of *Stowaway* MITEs in the rice genome. The observed excision of one *Stowaway* by two distinct transposases and the excision of two different *Stowaway*s by the same transposase suggest that cross-mobilization may be a major mechanism for the amplification of rice MITEs.

The differences in excision frequency between Ost35 and Osm14NA mirrored the difference in copy number between *Stowaway* MITEs and *Osmar* elements in the rice genomes (*10*). Several properties of the MITEs could explain the differential activity of Ost35 as compared with Osm14NA.

First, it is possible that the differences in size between Osm14NA and Ost35 (1004 versus 239 bp) may be a factor because increases in TE size has been shown to reduce transposition efficiency (*13*, *14*). Second, because transposition of *Mariner* elements requires the binding of transposase to transposon TIRs and/or subterminal regions to form synaptic complexes for subsequent excision and reintegration (*15*), any differential binding of *Osmar*14 transposase to the ends of Osm14NA and Ost35 may have affected their transposition activity. Ost35 has shorter TIRs than *Osmar*14 (20 versus 32 bp) and different subterminal sequences. Finally, Ost35 and Osm14NA also differ in their internal sequences, which may enhance or repress excision.

To investigate whether element size affects excision frequency, we shortened Osm14NA (1004 bp) to the length of Ost35 (239 bp) (now called Osm14NAS) (Fig. 2 and fig. S4). Relative to Osm14NA, the shorter Osm14NAS displayed weak but detectable excision activity (Fig. 2). Thus, size alone cannot account for the magnitude of excision activity of Ost35.

To investigate how transposase binding differed between elements, we examined the interaction of purified recombinant *Osmar*14 transposase with synthesized oligonucleotides corresponding to the terminal (32 bp) and subterminal (32 bp) regions of Ost35 and *Osmar*14 (Fig. 3A and fig. S4) in electrophoretic mobility shift assays. These experiments revealed differences in transposase affinity but not in the expected direction. For Ost35, the 5′ and 3′ terminal regions (abbreviated 5′T and 3′T, respectively, in Fig. 3A and fig. S4) each bound transposase equivalently. There was also some binding, albeit less efficiently, to each of the subterminal regions of Ost35 (5′ subT and

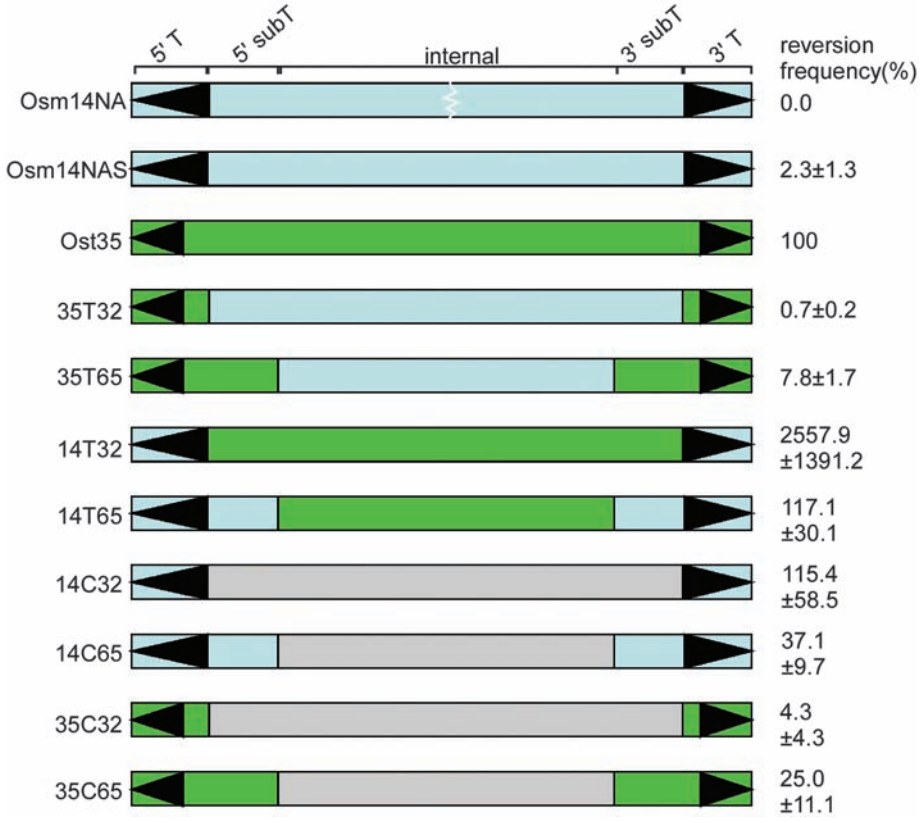

Fig. 2. Contribution of different regions of Osm14NAS and Ost35 to excision activity. *ADE2* reversion frequency is shown to the right of each construct. The chimeric constructs contain the following: 35T32, terminal 32 bp of Osm14NAS replaced by that of Ost35; 35T65, terminal 65 bp of Osm14NAS replaced by that of Ost35; 14T32, terminal 32 bp of Ost35 replaced by that of Osm14NAS; 14T65, terminal 32 bp of Ost35 replaced by that of Osm14NAS; 14C32, control sequence (coding sequence of *gfp*) flanked by terminal 32 bp of Osm14NAS; 14C65, control sequence flanked by terminal 65 bp of Osm14NAS; 35C32, control sequence flanked by terminal 32 bp of Ost35; and 35C65, control sequence flanked by terminal 65 bp of Ost35. Green represents regions derived from Ost35, blue represents regions derived from Osm14NAS, and gray represents regions derived from *gfp*.

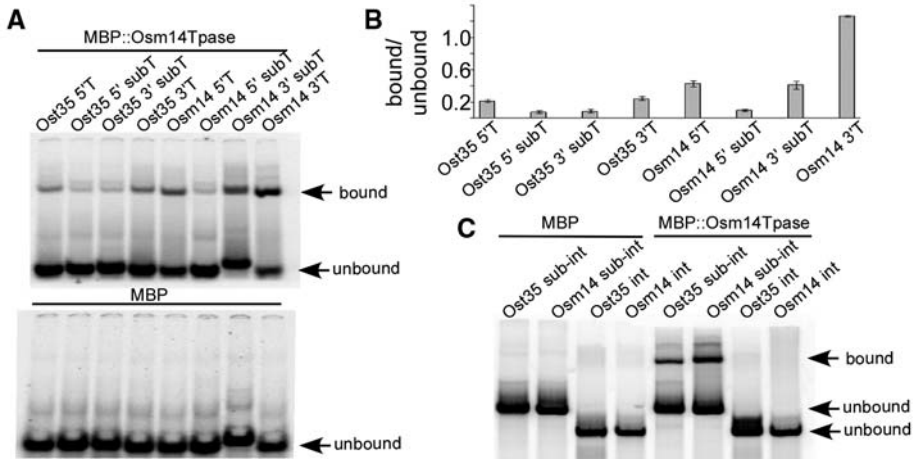

Fig. 3. *Osmar*14 transposase shows binding to regions of Ost35 and Osm14NAS. (**A**) Electrophoretic mobility shift assay (EMSA) of terminal and subterminal regions of Osm14NAS and Ost35. MBP, maltose binding protein control; MBP::Osm14Tpase, fusion protein of MBP and *Osmar*14 transposase; T, terminal 32 bp; subT, subterminal 32 bp. (**B**) Ratio of bound to unbound DNA. Error bars show SE of the mean for three independent events. (**C**) EMSA of the internal sequences of Ost35 and Osm14NAS (*12*). Int, internal sequences; sub-int, internal sequences with subterminal sequences attached were used as positive controls.

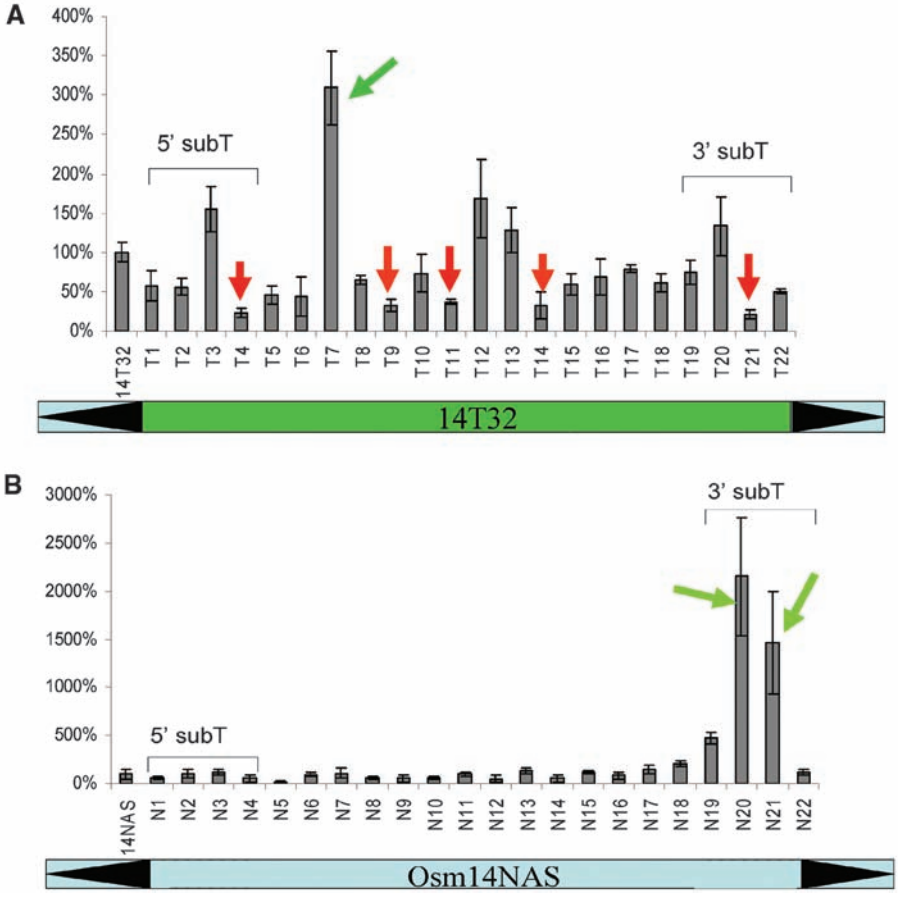

Fig. 4. Mutagenesis analyses of Ost35 and Osm14NAS internal sequences. (**A**) *ADE2* reversion frequency for mutations in the subterminal and internal sequences of Ost35. The template for mutagenesis was 14T32. (**B**) *ADE2* reversion frequency for mutations in the subterminal and internal sequences of Osm14NAS. Positions of mutations correspond to that on the diagram shown beneath each chart. T followed by a number indicates 14T32 mutated at the indicated site; N followed by a number indicates Osm14NAS mutated at the indicated site. Green arrows indicate positions of mutations that resulted in increased activity, and red arrows indicate mutations that resulted in decreased activity.

the 3′ subT in Fig. 3A and fig. S4). In contrast, both the terminal and subterminal regions of *Osmar*14 bound to transposase more strongly than the equivalent regions in Ost35. In addition, binding to *Osmar*14 was asymmetrical because sequences from the 3′ end of the element showed more binding affinity than those from the 5′ end. We detected no binding to the sequences internal to the subTs of either Ost35 or Osm14NA (Fig. 3, B and C, and fig. S4). Furthermore, when unlabeled Osm14NAS or Ost35 was used to compete with radiolabeled Osm14NAS, Ost35 did not outcompete Osm14NAS for transposase binding (fig. S5). These results suggest that the higher excision frequency of Ost35 is not due to an increased affinity for the *Osmar*14 transposase.

We swapped multiple regions between Osm14NAS and Ost35 and confirmed that the central region of Ost35 is involved in enhancing the frequency of excision (Fig. 2). However, this experiment showed, surprisingly, that despite the poor function of Osm14NAS in the excision assay, the replacement of the Ost35 TIRs by those of *Osmar*14 (a chimeric element we called 14T32) resulted in a ~25-fold increase in excision as compared with the original Ost35 transposon or a modified Ost35 with a different internal sequence of the same length (in this case, derived from the *gfp* gene). These data suggest that the function of the TIRs is normally suppressed in Osm14NAS (and also presumably in the natural *Osmar*14 element), whereas the function of the Ost35 TIRs is enhanced by the sequence between them. Further supporting this theory, we observed that the subTs of Osm14NAS represses excision when combined with either the *Osmar*14 TIRs, the equivalent regions of Ost35, or a different internal sequence (Fig. 2). Also, the region of Ost35 between the terminal sequences (32 bp) enhanced excision of adjacent TIRs by ~20-fold relative to the random internal sequence.

Taken together, these data support two general conclusions. For Osm14NAS, the extremely low excision frequency suggests that there is repression of the otherwise optimal *Osmar*14 TIRs by one or both of its subterminal regions. For Ost35, the high excision frequency most likely indicates that there is enhancement of the otherwise suboptimal Ost35 TIRs by part of or the entire Ost35 internal region.

We next performed site-directed mutagenesis so as to more precisely localize the regions responsible for the enhancement and repression of excision in the internal region of Ost35 and the Osm14NAS subTs, respectively. We used 14T32 and Osm14NAS constructs as the templates for mutagenesis. For each construct, we replaced consecutive blocks of eight nucleotides by the sequence ATTTAAAT (*Swa*I restriction site), resulting in 22 derivative constructs from each starting template. Among the mutant constructs derived from 14T32, a 75 to 80% decrease in excision activity was caused by mutations distributed throughout the Ost35 internal region, whereas a single mutation showed an approximately three-

fold increase (Fig. 4A). These data suggest that multiple motifs throughout the Ost35 internal region may promote excision by transposase probably through, for example, favorable DNA curvature or chromatin structure. In contrast, mutagenesis of Osm14NAS pinpointed the repressive region to the 3′ subterminal region where mutations resulted in up to a 20-fold increase in excision activity (Fig. 4B).

Our data support a model for the cross-mobilization of *Stowaway* elements by *Osmar* transposase and suggest how *Stowaway* MITEs may arise and amplify in the genome. Most plant genomes characterized to date, including rice, harbor relatively few *Mariner*-like elements (such as *Osmar*) but hundreds to tens of thousands of *Stowaway* MITEs (*10*, *16*, *17*). Our data suggest that the low copy number of *Osmar*14, and possibly other *Osmar*s, is due in part to a self-regulatory mechanism involving a repressive motif in their 3′ subterminal region. We speculate that this strategy limits the amplification of the elements, thereby attenuating their deleterious effects and facilitating their persistence in the genome.

The vertical persistence of DNA transposons has been hypothesized to be accompanied by diversification of transposase DNA-binding activities (*10*, *18*, *19*), suggesting that their sequence specificity undergoes episodic relaxation. This view is supported by the fact that *Osmar* transposases have surprisingly weak binding specificity (*20*) and can apparently cross-mobilize distantly related *Osmar*s (Fig. 1). Although the apparent promiscuity of *Osmar* transposases may facilitate their survival by buffering any potential impact of inactivating mutations (*18*), it may also allow parasitism by simpler transposons with similar binding sites, such as *Stowaway* MITEs. One factor underlying the success of *Stowaway* MITEs may be the fact that they have minimal cis-requirements for recognition by *Osmar* transposases, coupled to the presence of internal sequences that enhance excision. As short non-coding elements, *Stowaway*s may rapidly increase their copy number by tapping into a transposase source if and when it becomes available. In summary, MITE amplification may differ from previously postulated models of transposon invasion and provides an illustration of the complex ecosystem deployed within the genome. Because MITEs are widespread in eukaryotes, the fundamental principles outlined herein may be applicable to a broad range of organisms.

References and Notes

1. S. R. Wessler, T. E. Bureau, S. E. White, *Curr. Opin. Genet. Dev.* **5**, 814 (1995).
2. G. Yang *et al.*, *Plant Cell* **17**, 1559 (2005).
3. J. Piriyapongsa, I. K. Jordan, *PLoS One* **2**, e203 (2007).
4. C. Feschotte, X. Zhang, S. R. Wessler, in *Mobile DNA II*, N. Craig, R. Craigie, M. Gellert, A. Lambowitz, Eds. (American Society for Microbiology Press, Washington, DC, 2002), pp. 1147–1158.
5. T. Nakazaki *et al.*, *Nature* **421**, 170 (2003).
6. K. Kikuchi, K. Terauchi, M. Wada, H. Y. Hirano, *Nature* **421**, 167 (2003).
7. N. Jiang *et al.*, *Nature* **421**, 163 (2003).
8. K. Naito *et al.*, *Proc. Natl. Acad. Sci. U.S.A.* **103**, 17620 (2006).
9. N. Jiang, C. Feschotte, X. Zhang, S. R. Wessler, *Curr. Opin. Plant Biol.* **7**, 115 (2004).
10. C. Feschotte, L. Swamy, S. R. Wessler, *Genetics* **163**, 747 (2003).
11. G. Yang, C. F. Weil, S. R. Wessler, *Plant Cell* **18**, 2469 (2006).
12. Materials and methods are available as supporting material on *Science* Online.
13. L. R. Tosi, S. M. Beverley, *Nucleic Acids Res.* **28**, 784 (2000).
14. J. C. Way, N. Kleckner, *Genetics* **111**, 705 (1985).
15. C. Auge-Gouillou, B. Brillet, M. H. Hamelin, Y. Bigot, *Mol. Cell. Biol.* **25**, 2861 (2005).
16. C. Feschotte, S. R. Wessler, *Proc. Natl. Acad. Sci. U.S.A.* **99**, 280 (2002).
17. G. Menzel *et al.*, *Chromosome Res.* **14**, 831 (2006).
18. D. L. Hartl, A. R. Lohe, E. R. Lozovskaya, *Annu. Rev. Genet.* **31**, 337 (1997).
19. D. J. Lampe, K. K. Walden, H. M. Robertson, *Mol. Biol. Evol.* **18**, 954 (2001).
20. C. Feschotte, M. T. Osterlund, R. Peeler, S. R. Wessler, *Nucleic Acids Res.* **33**, 2153 (2005).

21. We thank C. F. Weil and D. J. Garfinkel for materials and technical assistance and J. Bennetzen, X. Zhang, and J. Leebens-Mack for discussion and insightful comments. This work was supported by NIH, the NSF Plant Genome Program, the University of Georgia Research Foundation, and the University of Toronto. Sequences for *Osmar* transposase coding sequences and their nonautonomous elements were deposited in GenBank (accession numbers GQ379705 to GQ379718 and GQ382183).

Supporting Online Material

www.sciencemag.org/cgi/content/full/325/5946/1391/DC1
Materials and Methods
Figs. S1 to S5
Table S1
References
Sequences and Primers

1 May 2009; accepted 16 July 2009
10.1126/science.1175688

The RNA-Binding Protein NANOS2 Is Required to Maintain Murine Spermatogonial Stem Cells

Aiko Sada,[1] Atsushi Suzuki,[2] Hitomi Suzuki,[3] Yumiko Saga[1,3,4]*

Stem cells give rise to differentiated cell types but also preserve their undifferentiated state through cell self-renewal. With the use of transgenic mice, we found that the RNA-binding protein NANOS2 is essential for maintaining spermatogonial stem cells. Lineage-tracing analyses revealed that undifferentiated spermatogonia expressing *Nanos2* self-renew and generate the entire spermatogenic cell lineage. Conditional disruption of postnatal *Nanos2* depleted spermatogonial stem cell reserves, whereas mouse testes in which *Nanos2* had been overexpressed accumulated spermatogonia with undifferentiated, stem cell–like properties. Thus, NANOS2 is a key stem cell regulator that is expressed in self-renewing spermatogonial stem cells and maintains the stem cell state during murine spermatogenesis.

Stem cells are essential for tissue homeostasis and regenerative responses to injury and disease. In the spermatogenic stem cell system, germ cell–intrinsic factors have an essential role in the maintenance of stem cells for the continuation of spermatogenesis throughout life (*1*–*5*). However, the previous loss-of-function studies have some limitations in terms of understanding the mechanism by which stem cells are lost upon the gene deletion, as it could be caused by cell death, defective self-renewal, premature differentiation, or other mechanisms.

For decades, the mammalian spermatogenic stem cell has been characterized by the morphological features of the spermatogonia. The spermatogonial types A_{single} (A_s; isolated single cells), A_{paired} (A_{pr}; chains of 2 cells), and $A_{aligned}$ (A_{al}; chains of 4, 8, 16 or 32 cells) are the most primitive germ cells observed in mature testes and are collectively described as undifferentiated spermatogonia. They give rise to differentiating spermatogonia, which undergo additional divisions and enter a differentiation pathway. It has been proposed that only A_s spermatogonia represent the stem cells (*6*–*8*); however, there is no A_s-specific molecular marker, and the presence of stem cells is assayed by long-term colony formation after the transplantation of candidate cells into recipient testes (*9*). For this reason, undifferentiated spermatogonia containing A_s to A_{al} are the smallest population proven to have the properties of stem cells.

Recently, two functionally distinct spermatogonial stem cell populations were identified in mice (*10*). One is the population that acts as the self-renewing stem cells (actual stem cells), and the other population possesses the potential to self-

[1]Department of Genetics, SOKENDAI, 1111 Yata, Mishima, Shizuoka 411-8540, Japan. [2]Interdisciplinary Research Center, Yokohama National University, 79-1 Tokiwadai, Hodogaya-ku, Yokohama 240-8501, Japan. [3]Department of Biological Sciences, Graduate School of Science, University of Tokyo, Hongo 7-3-1, Bunkyo-ku, Tokyo, 113-0033, Japan. [4]Division of Mammalian Development, National Institute of Genetics, 1111 Yata, Mishima 411-8540, Japan.

*To whom correspondence should be addressed. E-mail: ysaga@lab.nig.ac.jp

Supporting Online Material for

Tuned for Transposition: Molecular Determinants Underlying the Hyperactivity of a *Stowaway* MITE

Guojun Yang, Dawn Holligan Nagel, Cédric Feschotte, Charles N. Hancock, Susan R. Wessler*

*To whom correspondence should be addressed. E-mail: sue@plantbio.uga.edu

Published 11 September 2009, *Science* **325**, 1391 (2009)
DOI: 10.1126/science.1175688

This PDF file includes:

Methods and Materials

Plasmid construction and yeast excision assay

Exons of *Osmar* coding sequences, as determined by the alignment of *Osmar* transposase sequences, were amplified from rice genomic DNA (*Osmar*5, *Osmar*9, *Osmar*10, *Osmar*14) or BAC/PAC vectors (*Osmar1, Osmar17, Osmar19* from CUGI clone OSJNBa0051P13, OSJNBb0024B16 and OSJNBa0050F15 respectively, Clemson University Genomics Institute, Clemson, SC) before they were joined together with PCR via an overlapping region on the primers to obtain full length coding sequences. The single nucleotide deletion mutation close to the end of the first exon of *Osmar*14 was repaired based on the alignment of *Osmar* transposases using a PCR primer with the corrected sequence. The coding sequences for *Osmar*5 and *Osmar*10 were obtained as previously described (S*1*). Nonautonomous versions of the *Osmars* that served as transposase source were constructed by joining the fragments of ~450 bp from each end by PCR. Osm14NA (1004 bp) was further shortened to the size of Ost35 (239 bp) by a similar approach, resulting in Osm14NAS element. Because the 5'end of *Osmar*19 is missing in the sequenced rice genome, Osm19NA was generated with identical but inverted 5' and 3' ends. The *Stowaway* elements used in this study were chosen on the basis of their family diversity and then similarity to the consensus sequences of corresponding families was used. *Stowaway*s were first amplified from rice genomic DNA with PCR primers corresponding to the flanking sequences of each element extracted from rice genome sequence with a MITE Analysis Kit (MAK)(S*2*). Individual *Stowaway* sequences were subsequently amplified with element specific primers.

Transposase coding sequences were cloned into a pRS413 based vector, as described (S*3*). The nonautonomous *Osmar*s and *Stowaway*s were cloned into the *Hpa*I site inside the *ade*2 reporter gene on pWL89A (S*4*). Excision assays were performed, as described (S*3*). Genomic DNA of *ADE2* revertants was used as template for PCR to confirm TE excision with primers flanking TE donor sites. Genomic DNA blot analysis was performed, as described (S*3*). Sequences of TE elements and primers are included in this document.

Electrophoretic mobility shift assay (EMSA)

The coding sequence of the *Osmar*14 transposase was fused to the maltose binding protein gene on expression vector pMal-c2x (NEB, Ipswich, MA), expressed in *E.coli* (BL21) and purified with amylose beads (NEB) as was the maltose binding protein control. While the short fragments (32 bp) used for Fig. 2A were synthesized and annealed before performing the assay, the internal sequences or those including subterminal sequences used for Fig. 2C were obtained by PCR using full length Osm14NAS and Ost35 as templates. The *Osmar*14 3' subT fragment in Fig. 2A does not include six of the 12 bp low complexity poly C stretch between the 3' subT and 3' TIR. Double stranded DNA fragments were end labeled with P^{33} using T4 kinase (Invitrogen, Carlsbad, CA). Quantification of the intensity of the shifted bands was performed with Adobe Photoshop. The relative binding intensity was defined as the ratio of the signal intensity of the shifted band to that of the unbound DNA. Quantification was performed for three independent experiments.

Competition assay

Osm14NAS PCR products were labeled with P33 using T4 kinase (Invitrogen). Each reaction contained 15 ng of labeled DNA and 0.5 μg MBP (control) or *Osmar*14 TPase:MBP fusion protein in 15 mM Tris (pH 7.5), 0.1 mM EDTA, 1 mM DTT, 0.3

mg/ml BSA,0.1% NP-40, 10% glycerol and 33 μg/ml single-stranded DNA. Unlabeled Osm14NAS and Ost35 PCR products were used for competition at the following concentrations: 75 ng, 150 ng, 300 ng. Samples were separated on a 4% native polyacrylimade gel (0.5x TBE) after a 1 hour incubation at room temperature.

Construction of chimeric elements

To obtain the chimeric constructs in Figure 3 (those that have a "T" in their name, e.g. 14T32), PCR primers were designed to contain the terminal 32 bp of one element (e.g. Ost35) as 5' overhangs attached to the oligos priming into the subterminal region of the other element (e.g. Osm14NAS). Similarly, to obtain constructs bearing swapped terminal 65 bp regions, the 65 bp terminal sequences (e.g. of Ost35) were attached as 5' overhangs to the oligos priming into the internal sequences of the other element (e.g. Osm14NAS). Chimeric PCR products were then cloned into the *Hpa*I site in the *ade*2 reporter gene for use in the yeast excision assay. To construct control plasmids containing the terminal (32 or 65 bp) sequences of Osm14NAS or Ost35, a randomly chosen region in the green fluorescent protein gene (mGFP5-er) was used as template with chimeric primers designed in a similar way as that described for the construction of the chimeric versions of Ost35 and Osm14NAS.

Site-directed mutagenesis

For site-directed mutagenesis, primers (~45 nt) were designed to include ~18 nt on both sides of a mutation target site (8 nt), to be replaced with a *Swa*I site (ATTTAAAT). Mutagenesis was performed according to the manufacturer's manual with a QuikChange Mutisite-directed mutagenesis kit (Stratagene, La Jolla, CA). Mutant constructs were identified by the presence of a *Swa*I site through restriction enzymatic digestion (*Swa*I and *Sal*I) and/or sequencing. Primer sequences are included in this document.

Supplemental Figure Legends:

Fig. S1. *Osmar*s and *Stowaway*s in rice. (**A**) Approximate copy numbers of *Osmar* (autonomous and nonautonomous) and *Stowaway* elements in the sequenced rice genome (numbers in parenthesis) (*Oryza sativa ssp. japonica cv* nipponbare). The pie-chart is not drawn to scale as the proportion of *Osmar*s is one tenth of that shown. (**B**) Relationship of autonomous *Osmar*s, nonautonomous *Osmar*s, deletion derivatives and *Stowaway*s. CTCCCTCYGT is the terminal sequences shared among *Osmar*s and *Stowaway*s; black triangles represent TIRs; green regions in *Osmar*s represent transposase genes with introns (vertical white bars); red stars indicate nonsense or frame-shifting mutations; colored *Stowaway*s represents different families.

Fig. S2. (**A**) *ADE2* revertants following excision of Ost35 catalyzed by the *Osmar*14 transposase. The tpase source is shown in white letters; Donor indicates the element inserted into *ade2*. Each plate contains three sectors representing three independent events. (**B**) PCR analysis of the donor sites in *ADE2* revertants. C, plasmid control; PCR primer positions are shown in 1A. (**C**) DNA sequence of donor sites after excision of Ost35. The sequence of the donor site before excision is shown at the top and excision sites from independent *ADE2* revertants are below. (**D**) Genomic DNA blot analysis of *ADE2* revertants from Ost35 and 14T32. Yeast genomic DNA was digested with *Dra*I and separated by agarose gel electrophoresis. Radioisotope (P^{32}) labeled DNA fragment

corresponding to the sequence of Ost35 was used as probe. C, plasmid control that resulted in a single band of ~3 kb.

Fig. S3. Donor sites (**A**) and insertion sites (**B**) of OsmNAs and *Stowaway*s after transposition. The donor sites for Ost35 are shown in Fig. 1D. Red letters, target site duplications. The insertion sites of *Osmar*5 were previous determined (S*3*).

Fig. S4. Engineered internal deletion derivatives of *Osmar*14 and regions used for EMSA. Arrowheads, TIRs; vertical dotted lines, break points in Osm14NA and Osm14NAS. Regions used in EMSA shown in Fig. 2 are indicated for both Osm14NAS and Ost35.

Fig. S5. Competition assay between Osm14NAS and Ost35. Wedge, increasing amount of unlabeled DNA; Small arrowhead indicates where DNA was bound by transposase at one site; large arrowhead indicates where DNA was bound by transposase at multiple sites; lower band (no arrow), unbound labeled DNA. The entire Osm14NAS was end labeled with P33 radioisotope. Equal molar amounts of labeled DNA was added in each lane and equal molar amounts of unlabeled DNA was used in corresponding lanes of Osm14NAS and Ost35.

Table S1. *ADE2* reversion of nonautonomous *Osmar*s and *Stowaways*

Donor	Media	Transposase source					
		*Osmar*1	*Osmar*5	*Osmar*9	*Osmar*10	*Osmar*14	*Osmar*17
Ost8	YPD	212, 180, 240					124, 124, 40
	-ade	1, 0, 0					0, 1, 1
Ost16	YPD					48, 64, 56	
	-ade					0, 0, 1	
Ost35	YPD					176, 88, 168	
	-ade					588, 484, 195	
Osm1NA	YPD	-, -, 297					
	-ade	0, 0, 1					
Osm5NA	YPD		156, 228, 60				
	-ade		3, 32, 12				
Osm14NA	YPD						
	-ade						
Osm17NA	YPD		252, 328, 160				
	-ade		8, 12, 25				
Osm19NA	YPD			300, -, -	136, -, -	100, 284, 256	
	-ade			1, 0, 0	1, 0, 0	0, 0, 1	

The number of colonies on YPD media and revertants on media lacking adenine are shown only for the combinations that produced *ADE2* revertants. The cells in each galactose-induced colony were suspended in 50 µl of water and plated on media lacking adenine. An equal volume, but diluted $3.6x10^5$ times from the aforementioned cell suspension, was plated on YPD media to obtain the total number of viable cells in the galactose-induced colony. Each number separated by a comma is the number of colonies/revertants grown from one galactose-induced colony. The number of *ADE2*

revertants is shown beneath that on YPD plate correspondingly. "-", colonies too dense to get an accurate count (>500).

Supplemental References:

S1. C. Feschotte, M. T. Osterlund, R. Peeler, S. R. Wessler, *Nucleic Acids Res.* **33**, 2153 (2005).
S2. G. Yang, T. C. Hall, *Nucleic Acids Res.* **31**, 3659 (2003).
S3. G. Yang, C. F. Weil, S. R. Wessler, *Plant Cell* **18**, 2469 (2006).
S4. C. F. Weil, R. Kunze, *Nat. Genet.* **26**, 187 (2000).

Sequences and Primers

1. Accession numbers for *Osmar* transposase CDS and nonautonomous elements

Transposase	**Accession No**	**Sites for cloning**	**Size (bp)**
Osm1	GQ379705	S*pe*I, E*co*RI	1731
Osm5	GQ379706	B*am*H1, E*co*RI	1509
Osm9	GQ379707	B*am*HI, E*co*RI	1338
Osm10	GQ379708	E*co*RI, X*ho*I	1353
Osm14	GQ379709	B*am*HI, E*co*RI	1377
Osm17	GQ379710	B*am*H1, E*co*RI	1515
Osm19	GQ379711	B*am*HI, X*ho*I	1314
OsmarNA			
Osm1NA	GQ379712	H*pa*I	950
Osm5NA	GQ382183	H*pa*I	946
Osm9NA	GQ379713	H*pa*I	996
Osm10NA	GQ379714	H*pa*I	971
Osm14NA	GQ379715	H*pa*I	1004
Osm14NAS	GQ379716	H*pa*I	239
Osm17NA	GQ379717	H*pa*I	1044
Osm19NA	GQ379718	H*pa*I	945

2. Accession numbers and positions for *Stowaway*s used in this study

Stowaways	**Accession No**	**Position**	**Length (bp)**
Ost5	AP003455	161027 to 161280	254
Ost8	AP006237	115925 to 115670	256
Ost10	BX548156	36272 to 36014	259
Ost11	AC136786	39608 to 39320	289
Ost13	AP005259	120349 to 120599	251
Ost14	AP004553	137117 to 137371	255
Ost15	AC119149	42651 to 42507	143
Ost16	AC130724	64038 to 63815	224
Ost18	AC091122	121581 to 121797	217
Ost20	AC107314	3947 to 4224	278
Ost24	AC079179	54121 to 54357	237
Ost28	AP005586	90538 to 90794	257
Ost34	AC034258	81114 to 80858	255
Ost35	AP003270	47168 to 46930	239
Ost42	AP003832	94101 to 94341	241
Ost46	AP004891	64239 to 64383	145
Ost52	AC108224	15931 to 15697	233

3. Primers for *Osmar* coding sequence cloning

osmar19-BamHI for	actatggatccatgcacggtagtgtttttttttccatttagaacatgc
osmar19-XhoI rev	atcaactcgagtcatctagcaaagatggttcgcaaggga
osmar19-exon1 rev	ccgaatactccatgaatgcctcttccactgttggaactagagcttctattgtttttg
osmar19-exon2 for	ctagttccaacagtggaagaggcattcatggagtattcggcacacaaag
osmar14-BamHI for	actatggatccatgcaagagtacggcgtgtatgcgg
osmar14-EcoRI rev	atcaagaattcttactgcacttggttggctaatgctgttg
osmar14-exon1 rev	ttgtcctttgcgctggttcctttctggtgaaaggccacaatcctatcttg
osmar14-exon2 for	tgtggcctttcaccagaaaggaaccagcgcaaaggacaagtcataatagac
osmar17-BamHI for	actatggatccatggagcatgacctggatatgcatgca
osmar17-EcoRI rev	atcaagaattcttagttgcctagaagttgtatgactttctcatacaactg
osmar17-exon2 for	gaggaacaagaaattcaactagacaatgacaatgaattgcaacatgagctgg
osmar17-exon2 rev	ttctcctttgtgcgggttcctttctaacaaaaggccaaatgcctatcttaccatcaaaag
osmar17-exon3 for	atttggccttttgttagaaaggaacccgcacaaaggagaagccgta
Osm10 for EcoRI	tcaatggaattcatgcatgccaaccatagtatagcctgca
Osm10 rev XhoI	attctactcgagtcgcccttactatgtattgatgaaatctaccgcatc
osmar9-BamHI for	actatggatccatgcatatatataaatattttctttgtgcagatactcaacaagac
osmar9-EcoRI rev	atcaagaattcctagttcaacaaggtctgcataaccttgttg
osmar9-exon1 rev	ctactcctttgtgctggttccttcctaacaaagggccatattcctattttgc
Osmar9-exon2 for	tatggccctttgttaggaaggaaccagcacaaaggagtagtcgca
osmar1-SpeI for	actagactagtatgccattctttagaaccccgttgagc
osmar1-EcoRI rev	atcaagaattcttacctgagataattgttagcattatttactgacttagcatcacac

4. Primers for OsmNA cloning

Osm1 P-TA-5' TIR for	/5'phos/tactccctccgtttcgttttgtttgtcgtttc
Osm1 P-TA-3' TIR rev	/5'phos/tactccctccgtttcgttttgtttgtcgct
Osm5 P-TA-5' TIR for	/5'phos/tactccctccgtcccacaaaacatgac
Osm5 P-TA-3' TIR rev	/5'phos/tactccctccgtcccacaaaacctgcc
Osm9 P-TA-5' TIR for	/5'phos/tactccctccgtcccacattatatgggactg
Osm9 P-TA-3' TIR rev	/5'phos/tactccctccgtcccatattatatgggattagaggtt
Osm10 P-TA-5' TIR for	/5'phos/tactccctccgttccttaatatagagcgtgg
Osm10 P-TA-3' TIR rev	/5'phos/tactccctccgttccttaatatagggcgtaac
Osm14 P-TA-5' TIR for	/5'phos/tactccctccgtcccagaaagaagggattc
Osm14 P-TA-3' TIR rev	/5'phos/tactccctccgtcccagaaagaagcgatttct
Osm17 P-TA-5' TIR for	/5'phos/tactccctccgtcccagaaaggaggacgt
Osm17 P-TA-3' TIR rev	/5'phos/tactccctccgtcccagaaaggaggacgt
Osm19 P-TA-TIR	/5'phos/tactccctccgtatcacaattagaagatgttttgcgt
Osm1 5' middle rev	gctgatacatggcgtggagggtggtggcaaatcgcaaagaacgc
Osm1 3' middle for	cctccacgccatgtatcagcctgc
Osm9 5' middle rev	atcaaggttgagatcaggaatctcatattcctcttcttcc
Osm9 3' middle for	ttcctgatctcaaccttgattacctggacgttgaacttgacgaaggc
Osm10 5' middle rev	ggtggatttagatcaaaaccggccattacatacg
Osm10 3' middle for	ttttgatctaaatccaccacacggagcgtacgagcatgagcga
Osm14 5' middle rev	cgttcatggaagcggactgctgcttcttcagccactgcttca
Osm14 3' middle for	ccgcttccatgaacgctgctaccga
Osm17 5' middle rev	tgatgatggaggcggaaacttcaggtaaagcccctccatcttcct

Osm17 3' middle for	agtttccgcctccatcatcacctcca
Osm19 middle long	ttctcggcagtgagttcacatttgcgcttc
Osm19 middle short	actcactgccgagaaggaaccgaggagtgcgaagttaatacagc
Osm14NAS internal 5' rev	ctttatttgtacctaatgattaggtgtactagtactgagggtagtttag
Osm14NAS internal 3' for	cctaatcattaggtacaaataaagtattattgcccacatatgatgc

5. Primers for *Stowaway* cloning

First PCR (flanking)

Os10_flank for	gaaaaaaattttagtagggtagatcaa
Os10_flank rev	catgtttgtgaaatgacatatcaca
Os11_flank for	ttacaatgtgctctatgtcttttac
Os11_flank rev	caattgactaaggtctttatgttaa
Os13_flank for	ggtgagatttatgtttggtttttac
Os13_flank rev	gtaagtagaatgaacattagtatct
Os14_flank for	tcagaaaatattgttagtgtcctta
Os14_flank rev	ggccaaccgatccttagtacacaaa
Os15_flank for	gaagcggtgcacaaatgtaattgtg
Os15_flank rev	aggagcagctttttgccatatcagg
Os16_flank for	gcctgttactagttccttgtgcaat
Os16_flank rev	tgttagattcactatataaacctga
Os18_flank for	tcctaaaatataagcgtttgttagc
Os18_flank rev	cccaaaatataaatattttagctaaatcg
Os20_flank for	cttctttttttttttcaccaaaagagg
Os20_flank rev	gacacattctgtagtataaaatttag
Os24_flank for	cacacttcatctaattattctcatc
Os24_flank rev	gaggttggcacgggaattaaaaaaa
Os28_flank for	ggactctttttttatttatttaattgaatac
Os28_flank rev	ggtgcctccccacaaccaacaccta
Os34_flank for	ctgctataattctgtactattgtta
Os34_flank rev	gaatttcttgtggatctaataaaaatg
Os35_flank for	tactgttctgcaaaggactaggata
Os35_flank rev	gcctcgtgaaggtgctgagattacc
Os42_flank for	taatttctgaaatcatgcaatgcag
Os42_flank rev	ccagtagctcccataattgatacattt
Os46_flank for	aaaagtaggtgggtttattagtgcag
Os46_flank rev	catgttttggctgacttttgactca
Os5_flank for	agaagggcccaatccaagttgcaaa
Os5_flank rev	gttggtttctaatcttgttatcttattgc
Os52_flank for	gctgtatgcagtagaaaagaaatctac
Os52_flank rev	gttgttatcaaaagatgaccaggtaga
Os8_flank for	atcaagtttgaccaagtttatagaaaaatatat
Os8_flank rev	attttgataatatgtttgttttgtgttgaaaatag

Second PCR (TIR regions)

Os10_tir_for_code	/5’phos/tactccctccgtactcgtaaaa
Os10_tir_rev_code	/5’phos/tactccttccgtactcataaag
Os11_tir_for_code	/5’phos/tactccctccatctacttttaa
Os11_tir_rev_code	/5’phos/tactccctccatctacttttga

Os13_tir_code	/5’phos/tactccctccatcccaaaatat
Os14_tir_for_code	/5’phos/tactccctccatccacaaaagt
Os14_tir_rev_code	/5’phos/tactctctccatccacaaaagt
Os15_tir_code	/5’phos/tactccctccgtcccagaatat
Os16_tir_for_code	/5’phos/tactccctccgtcccagaatat
Os16_tir_rev_code	/5’phos/tactccctccgtcccaaaatat
Os18_tir_for_code	/5’phos/tactacctccgtctcaaaatat
Os18_tir_rev_code	/5’phos/tacttcctccgtcccaaaatgt
Os20_tir_for_code	/5’phos/tacctccatcccataaaaattg
Os20_tir_rev_code	/5’phos/tacctccgtcccataaaaattg
Os24_tir_for_code	/5’phos/tactacctccgtcccaaaataa
Os24_tir_rev_code	/5’phos/tacctccatcccaaaataattg
Os28_tir_for_code	/5’phos/tactccctccatcccataatat
Os28_tir_rev_code	/5’phos/tactccctctatcccataatat
Os34_tir_for_code	/5’phos/tactccctctgtcccaaattat
Os34_tir_rev_code	/5’phos/tactccatccgtcccaaattat
Os35_tir_for_code	/5’phos/tactccctccgtcccacaaaaa
Os35_tir_rev_code	/5’phos/tactccctccgtcccaaaaaaa
Os42_tir_for_code	/5’phos/tactccctccgtcccaaaataa
Os42_tir_rev_code	/5’phos/tactccctctgtcccgtaataa
Os46_tir_for_code	/5’phos/tactccctctgtcccaaaatat
Os46_tir_rev_code	/5’phos/tactccctccgtcccataatat
Os5_tir_for_code	/5’phos/tactccctccatttcaggttat
Os5_tir_rev_code	/5’phos/tactccctccgtttcaggttat
Os52_tir_for_code	/5’phos/tactccatccgtcctattttaa
Os52_tir_rev_code	/5’phos/tactccctccgtcccaatttaa
Os8_tir_code	/5’phos/tactccctccgtcccaaaatat

6. Primers for TIR swapping

Osm14NA TIR 5'-32-ost35intl	/5phos/tactccctccgtcccagaaagaagggattcctggcatcccgaggtgaaattagt
Ost35 TIR 3'-32-osm14intl	/5phos/tactccctccgtcccaaaaaaactcaacttctacgggggggggagactttgtc
Ost35 TIR 5'-32-osm14intl	/5phos/tactccctccgtcccacaaaaaatacattcctagaagcccaaggtagttttagg
Osm14NA TIR 3'-32-ost35intl	/5phos/tactccctccgtcccagaaagaagcgatttctggagtttgaattttgtcccata
Osm14NA TIR 5'-65-ost35intl	/5phos/tactccctccgtcccagaaagaagggattcctggaagcccaaggtagttttaggacaaagagcaaaagacaaaaataccttaatca
Ost35 TIR 5'-65-osm14intl	/5phos/tactccctccgtcccacaaaaaatacattcctagcatcccgaggtgaaattagtggagatggagaatggctaaactaccctcagtac
Osm14NA TIR 3'-65-ost35intl	/5phos/tactccctccgtcccagaaagaagcgatttctgggggggggggggagactttgtcccaaaaaaaaaagctaccatcctacctaccctca
Ost35 TIR 3'-65-osm14intl	/5phos/tactccctccgtcccaaaaaaactcaacttctacagtttgaattttgtcccataaaaaaccactttcgattcgtgcacaaaacacca
Ost35 TIR 5'-32-GFPintl1	/5phos/tactccctccgtcccacaaaaaatacattcctagaagctcatcatgtttgtatagttc
Ost35 TIR 3'-32-GFPintl1	/5phos/tactccctccgtcccaaaaaaactcaacttctacaaatactccaattggcgatggccct
Ost35 TIR 5'-65-GFPintl1	/5phos/tactccctccgtcccacaaaaaatacattcctagcatcccgaggtgaaattagtggagatggagaatatccatgccatgtgtaatcccag
Ost35 TIR 3'-65-GFPintl1	/5phos/tactccctccgtcccaaaaaaactcaacttctacagtttgaattttgtcccataaaaaaccactttcgtccttttaccagacaaccatta
Osm14 TIR 5'-32-GFPintl1	\5phos\tactccctccgtcccagaaagaagggattcctggaagctcatcatgtttgtatagttc
Osm14 TIR 3'-32-GFPintl1	\5phos\tactccctccgtcccagaaagaagcgatttctggaaatactccaattggcgatggccct
Osm14 TIR 5'-65-GFPintl1	\5phos\tactccctccgtcccagaaagaagggattcctggaagcccaaggtagttttaggacaaagagcaaaaatccatgccatgtgtaatcccag
Osm14 TIR 3'-65-GFPintl1	\5phos\tactccctccgtcccagaaagaagcgatttctgggggggggggggagactttgtcccaaaaaaaaagcgtccttttaccagacaaccatta

7. Primers for site directed mutagenesis

14T32_int_mut1	cagaaagaagggattcctggatttaaatggtgaaattagtggagatgg
14T32_int_mut2	atacattcctagcatcccgaatttaaattagtggagatggagaatgac
14T32_int_mut3	ctagcatcccgaggtgaaatatttaaatatggagaatgacaaaaatac
14T32_int_mut4	ccgaggtgaaattagtggagatttaaattgacaaaaataccttaatc
14T32_int_mut5	aaattagtggagatggagaaatttaaatatacctttaatcattgaaaa
14T32_int_mut6	ggagatggagaatgacaaaaatttaaataatcattgaaaaaatagtaa
14T32_int_mut7	agaatgacaaaaataccttattaaataaaaaatagtaagagtgata
14T32_int_mut8	aaaaataccttaatcattgatttaaatgtaagagtgataggtaggta
14T32_int_mut9	ctttaatcattgaaaaaataatttaaatgataggtaggtaaagagtat
14T32_int_mut10	ataccttaatcattgaaaaaatagtaagagtatttaaatggtaaagagtattgaaggaataaaatttctcg
14T32_int_mut11	aatagtaagagtgataggtaatttaaatgtattgaaggaataaaattt
14T32_int_mut12	gagtgataggtaggtaaagaatttaaatggaataaaatttctcgtttt
14T32_int_mut13	ggtaggtaaagagtattgaaatttaaatatttctcgttttacgtgctg
14T32_int_mut14	aagagtattgaaggaataaaatttaaatttttacgtgctgagggtagg
14T32_int_mut15	tgaaggaataaaatttctcgatttaaatgctgagggtaggtaggatgg
14T32_int_mut16	taaaatttctcgttttacgtatttaaattaggtaggatggtagaaagt
14T32_int_mut17	ctcgttttacgtgctgagggatttaaatatggtagaaagtggtttttt
14T32_int_mut18	acgtgctgagggtaggtaggatttaaataagtggtttttatgggaca
14T32_int_mut19	agggtaggtaggatggtagaatttaaatttttatgggacaaaattcaa
14T32_int_mut20	taggatggtagaaagtggttatttaaatgacaaaattcaaactgtaga
14T32_int_mut21	tagaaagtggtttttatggatttaaattcaaactgtagaagttgagt
14T32_int_mut22	ggtttttatgggacaaaatatttaaatcagaaatcgcttctttctgg
14NAS_int_mut1	cagaaagaagggattcctggatttaaatggtagttttaggacaaagag
14NAS_int_mut2	agggattcctggaagcccaaatttaaattaggacaaagagcaaaaggc
14NAS_int_mut3	ctggaagcccaaggtagtttatttaaatagagcaaaaggctaaactac
14NAS_int_mut4	ccaaggtagttttaggacaaatttaaataggctaaactaccctcagta
14NAS_int_mut5	gttttaggacaaagagcaaaatttaaatctaccctcagtactagtaca
14NAS_int_mut6	acaaagagcaaaaggctaaaatttaaatagtactagtacacctaatca
14NAS_int_mut7	caaaaggctaaactaccctcatttaaattacacctaatcattaggtac
14NAS_int_mut8	taaactaccctcagtactagatttaaatatcattaggtacaaataaag
14NAS_int_mut9	cctcagtactagtacacctaatttaaatgtacaaataaagtattattg
14NAS_int_mut10	ctagtacacctaatcattagatttaaataaagtattattgcccacata
14NAS_int_mut11	cctaatcattaggtacaaatatttaaatattgcccacatatgatgcga
14NAS_int_mut12	ttaggtacaaataaagtattatttaaatcatatgatgcgacacagata
14NAS_int_mut13	aaataaagtattattgcccaatttaaatgcgacacagataaaatatct
14NAS_int_mut14	tattattgcccacatatgatatttaaatgataaaatatctggtgtttt
14NAS_int_mut15	cccacatatgatgcgacacaatttaaatatctggtgttttgtgcacga
14NAS_int_mut16	tgatgcgacacagataaaatatttaaatttttgtgcacgaatcgcttt
14NAS_int_mut17	cacagataaaatatctggtgatttaaatacgaatcgctttttttttgg
14NAS_int_mut18	aaatatctggtgttttgtgcatttaaatctttttttttgggacaaagt
14NAS_int_mut19	ggtgttttgtgcacgaatcgatttaaatttgggacaaagtctcccccc
14NAS_int_mut20	gtgcacgaatcgctttttttatttaaataagtctccccccccccccag
14NAS_int_mut21	atcgctttttttttgggacaatttaaatcccccccccccagaaatcgct
14NAS_int_mut22	ttttttgggacaaagtctccatttaaatccagaaatcgcttctttctg

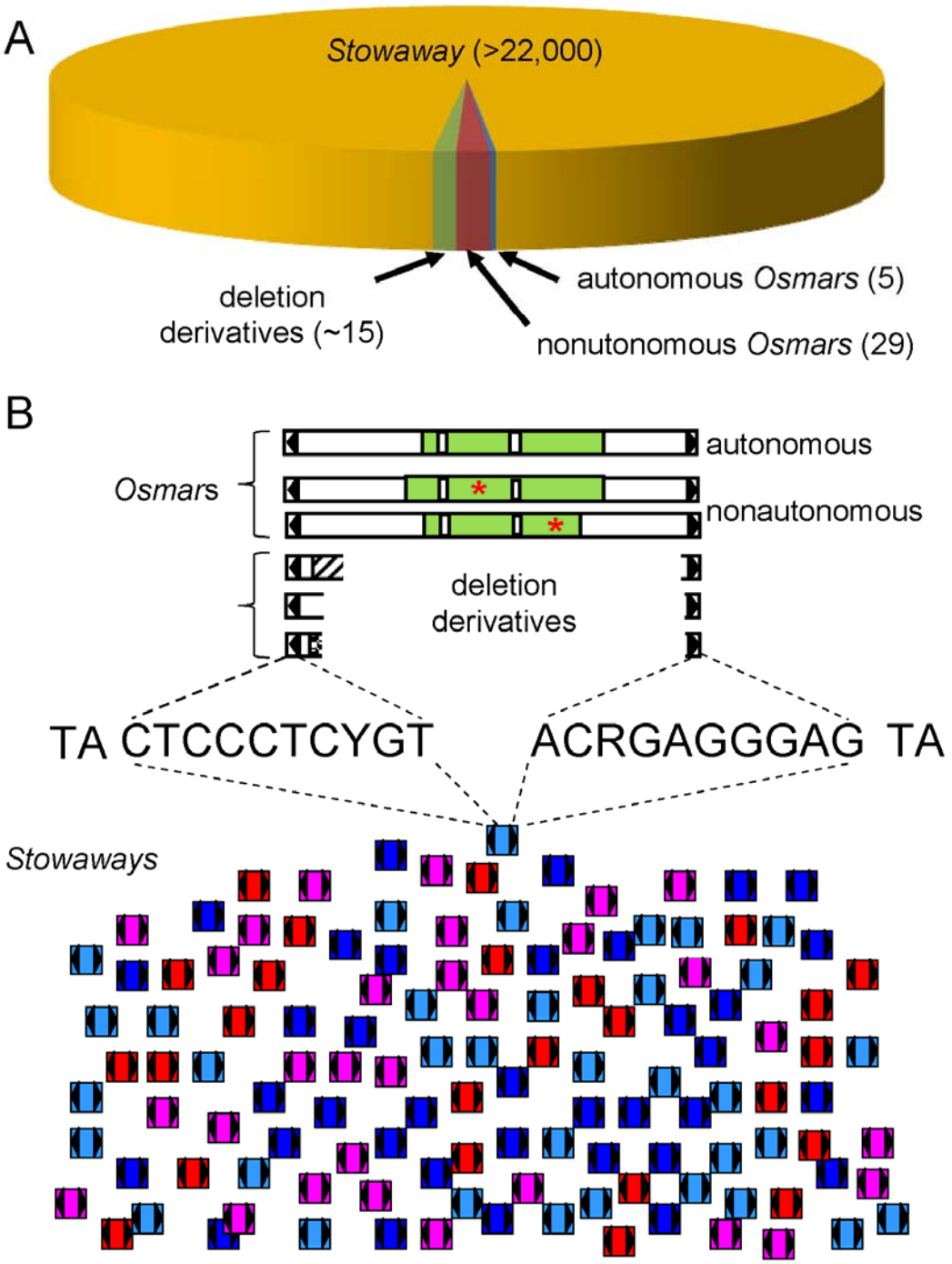
A
Stowaway (>22,000)
deletion
derivatives (~15)
autonomous Osmars (5)
nonutonomous Osmars (29)
B
Osmars
autonomous
nonautonomous
deletion
derivatives
TA CTCCCTCYGT
ACRGAGGGAG TA
Stowaways

Fig S1

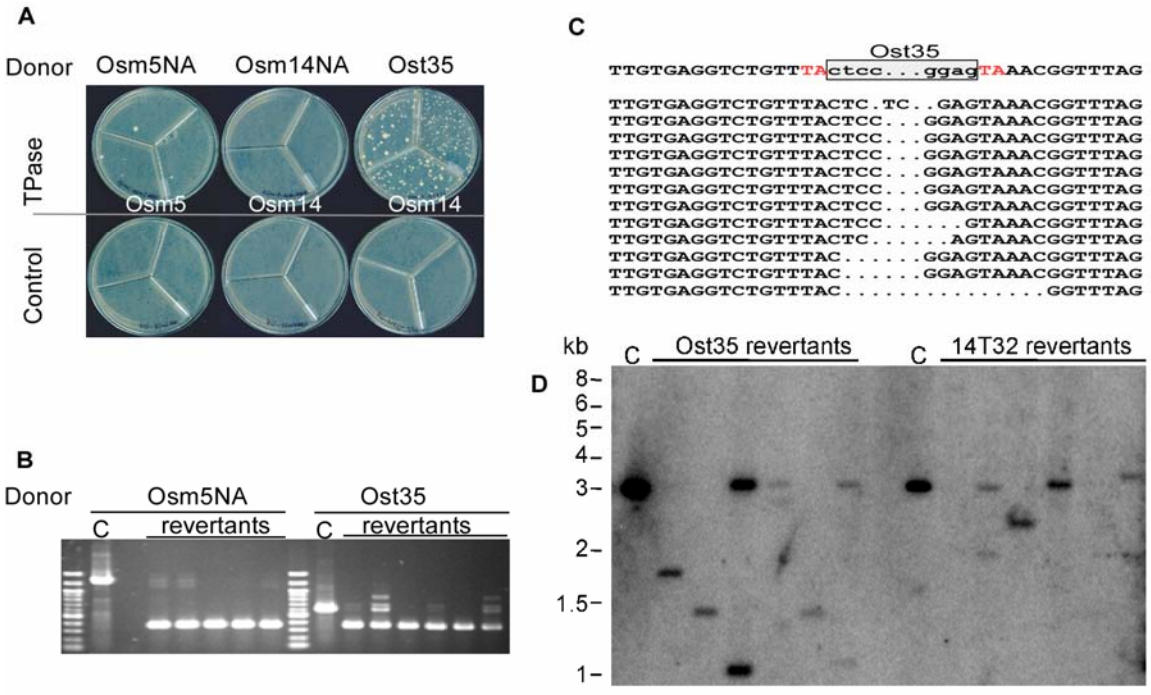
A
Donor
Osm5NA
Osm14NA
Ost35
TPase
Control
Osm5
Osm14
Osm14
B
Donor
Osm5NA
Ost35
C
revertants
C
revertants
C
Ost35
TTGTGAGGTCTGTTTACTCC...GGAGTAAACGGTTTAG
TTGTGAGGTCTGTTTACTC.TC..GAGTAAACGGTTTAG
TTGTGAGGTCTGTTTACTCC...GGAGTAAACGGTTTAG
TTGTGAGGTCTGTTTACTCC...GGAGTAAACGGTTTAG
TTGTGAGGTCTGTTTACTCC...GGAGTAAACGGTTTAG
TTGTGAGGTCTGTTTACTCC...GGAGTAAACGGTTTAG
TTGTGAGGTCTGTTTACTCC...GGAGTAAACGGTTTAG
TTGTGAGGTCTGTTTACTCC.....GTAAACGGTTTAG
TTGTGAGGTCTGTTTACTC.....AGTAAACGGTTTAG
TTGTGAGGTCTGTTTAC.....GGAGTAAACGGTTTAG
TTGTGAGGTCTGTTTAC.....GGAGTAAACGGTTTAG
TTGTGAGGTCTGTTTAC.....GGTTTAG
D
kb
C
Ost35 revertants
C
14T32 revertants
8
6
5
4
3
2
1.5
1

Fig S2

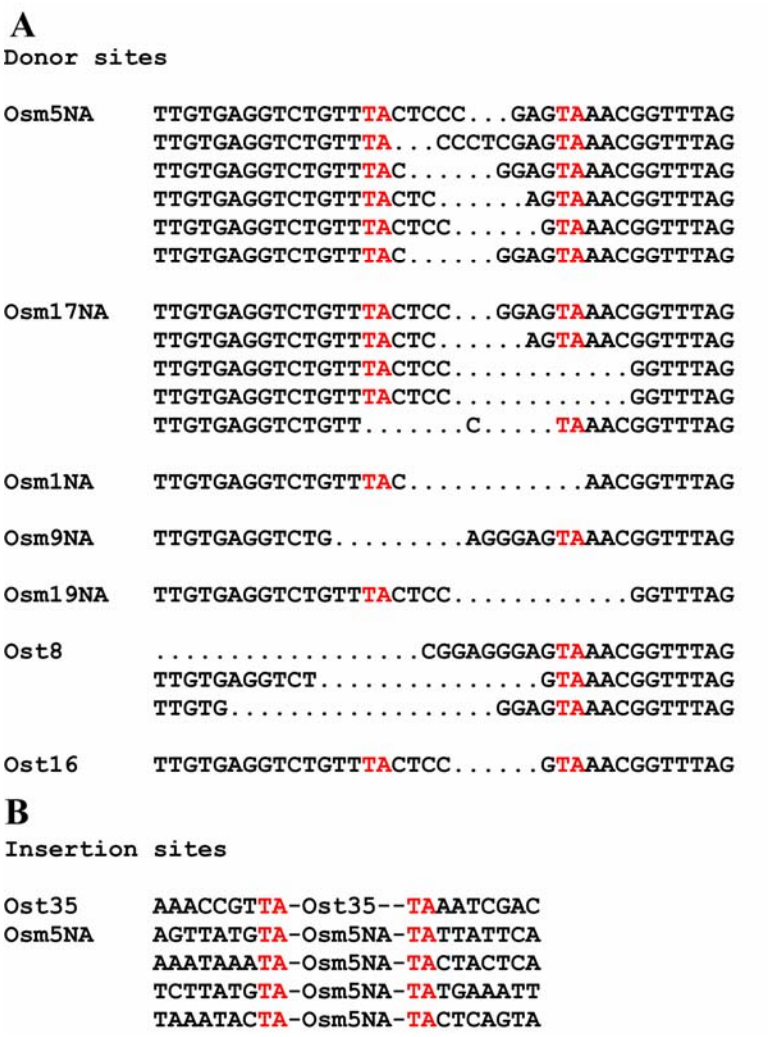
A
Donor sites
Osm5NA TTGTGAGGTCTGTTTACTCCC...GAGTAAACGGTTTAG
TTGTGAGGTCTGTTTA...CCCTCGAGTAAACGGTTTAG
TTGTGAGGTCTGTTTAC......GGAGTAAACGGTTTAG
TTGTGAGGTCTGTTTACTC......AGTAAACGGTTTAG
TTGTGAGGTCTGTTTACTCC......GTAAACGGTTTAG
TTGTGAGGTCTGTTTAC......GGAGTAAACGGTTTAG
Osm17NA TTGTGAGGTCTGTTTACTCC...GGAGTAAACGGTTTAG
TTGTGAGGTCTGTTTACTC......AGTAAACGGTTTAG
TTGTGAGGTCTGTTTACTCC.....GGTTTAG
TTGTGAGGTCTGTTTACTCC.....GGTTTAG
TTGTGAGGTCTGTT.......C.....TAAACGGTTTAG
Osm1NA TTGTGAGGTCTGTTTAC.....AACGGTTTAG
Osm9NA TTGTGAGGTCTG.....AGGGAGTAAACGGTTTAG
Osm19NA TTGTGAGGTCTGTTTACTCC.....GGTTTAG
Ost8 .....CGGAGGGAGTAAACGGTTTAG
TTGTGAGGTCT.....GTAAACGGTTTAG
TTGTG.....GGAGTAAACGGTTTAG
Ost16 TTGTGAGGTCTGTTTACTCC......GTAAACGGTTTAG
B
Insertion sites
Ost35 AAACCGTTA-Ost35--TAAATCGAC
Osm5NA AGTTATGTA-Osm5NA-TATTATTCA
AAATAAATA-Osm5NA-TACTACTCA
TCTTATGTA-Osm5NA-TATGAAATT
TAAATACTA-Osm5NA-TACTCAGTA

Fig S3

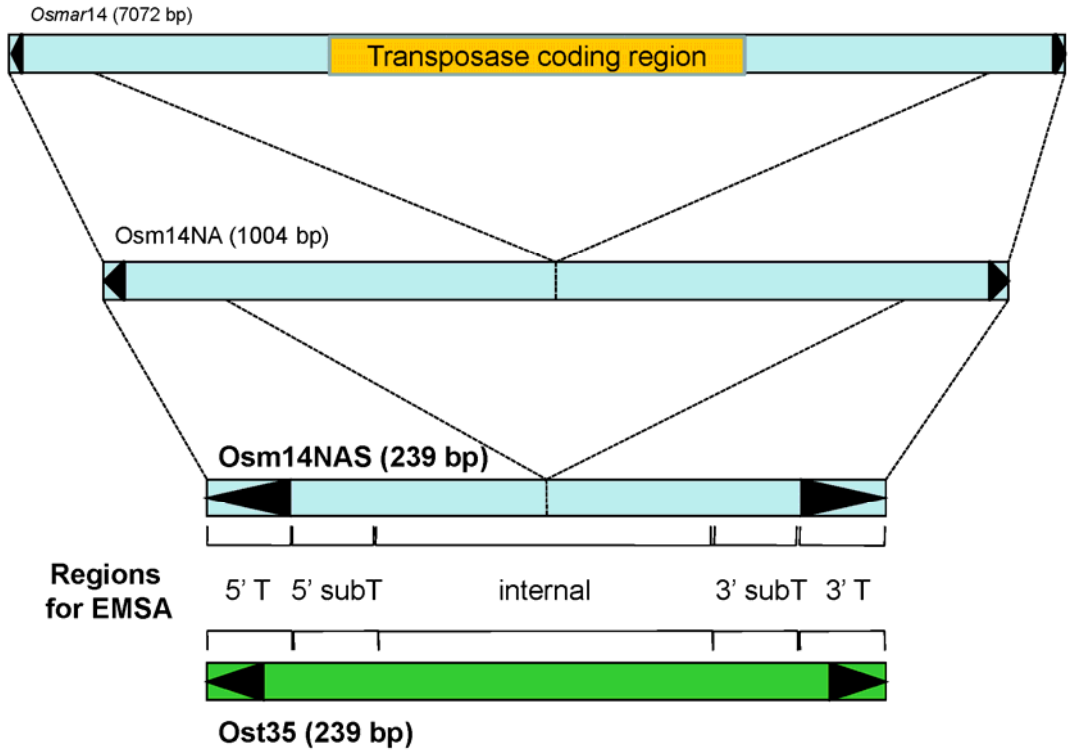
Osmar14 (7072 bp)
Transposase coding region
Osm14NA (1004 bp)
Osm14NAS (239 bp)
Regions for EMSA
5' T
5' subT
internal
3' subT
3' T
Ost35 (239 bp)

Fig S4

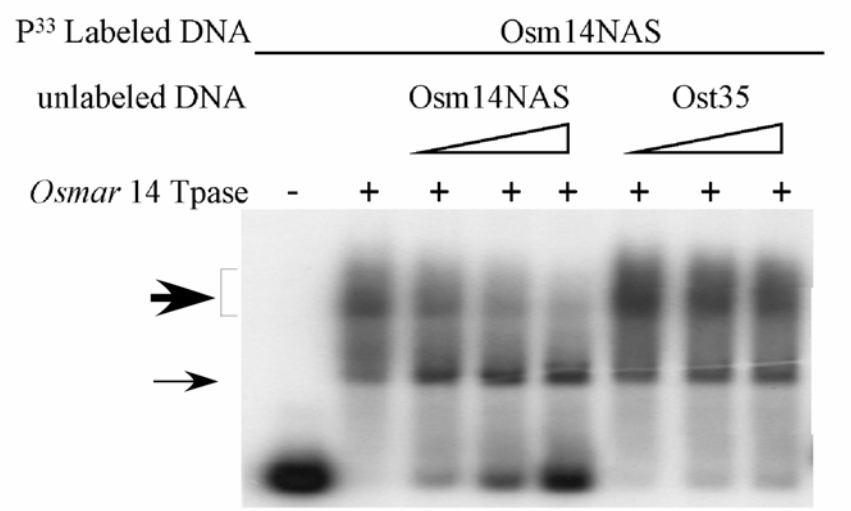
P33 Labeled DNA
Osm14NAS
unlabeled DNA
Osm14NAS
Ost35
Osmar 14 Tpase
- + + + + + + +

Fig S5